MULTIFERROIC THIN FILMS

NS190 Paper

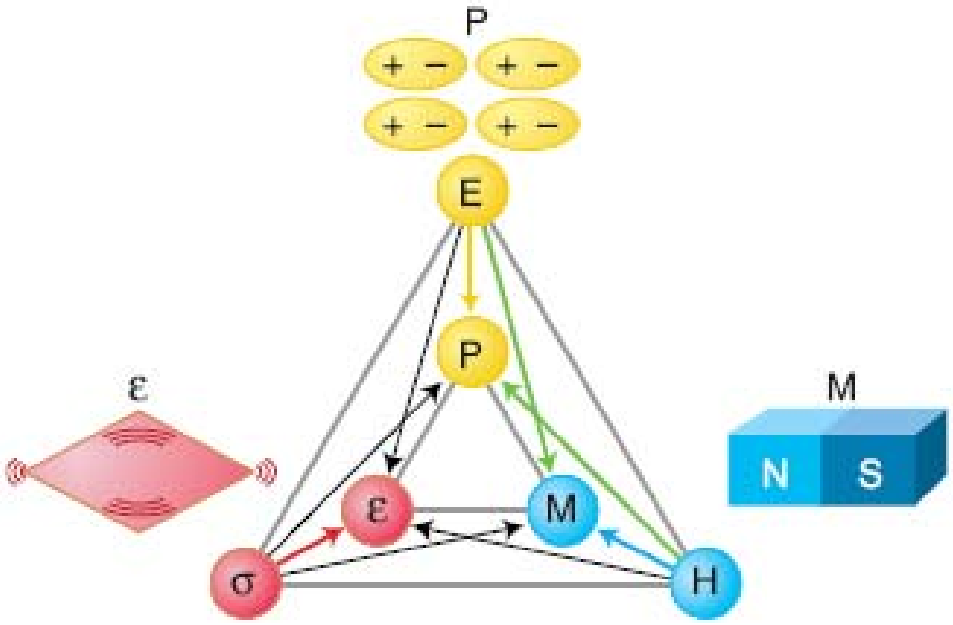

Taken from Science magazine ,Volume 309, July 2005 , page 391

Written by Arramel (1582585)
Under supervision of Beatriz Noheda

MSC plus
Materials Science Centre

Rijks*universiteit* Groningen

Abstract

Magnetic and ferroelectric materials have greatly contributed to the world of research and technology. Many applications have been introduced at many different scales from giant transformers to non-volatile memory devices. Multiferroic materials simultaneously combined ferroelectric and ferromagnetic within one phase. In order to understand multiferroic behavior, several mechanisms had been introduced for rare-earth manganites and other exotic oxides. Unfortunately, there are very few materials that possess both properties in the same time. Further, to increase the number of available materials and to improve the electromagnetic coupling on the existing ones, scientists are starting to synthesize them in thin film form. In this way the strain due to the substrate on to which the film is deposited acts as an extra degree of freedom. Recently, some of the publications on thin film had been conducted to investigate the effect of strain on the functional properties (magnetic, ferroelectric and magneto-electric) of these fascinating materials.

Contents

1. Rich and Fascinating Properties of Multiferroics

Multiferroic materials have attracted many scientists since the discovery of their ancestor nickel boracite ($Ni_3B_7O_{13}I$)[1]. Nowadays people are trying to find a simpler structure, for instance among the perovskite oxides, in order to have easier access to their fundamental behavior. These materials can exhibit magnetism and ferroelectricity simultaneously within one phase. The coupling between the magnetization and electric polarization gives place to magnetoelectric (ME) effects, which offer an extra degree of freedom in the design of conventional actuators or storage devices. Interesting applications can be thought of using this coupling, for instance, novel multi-state memory devices[2] that allow to write data using electric fields and to read out by means of magnetic fields. Unfortunately, these interesting materials are rare and difficult to find either in natural forms or as synthesized products. In this paper, I would like to give an overview about the state of art of research in multiferroics. For that I will present a general introduction of the fundamental properties that arise from the combination of ferromagnetism and ferroelectricity, and how these properties can be enhanced in thin films. At the end, general remarks about the future prospects of multiferroics will be shortly made.

1.1. Ferromagnets and Ferroelectrics (ferroic materials)

Ferromagnetic materials have a spontaneous magnetization (at H= 0) that can be aligned and switched with a magnetic field. Unlike in paramagnetic or diamagnetic materials, the response of the magnetization to the field is highly non-linear and presents hysteresis (Figure 1). The most common examples of ferromagnets are metals like Co, Ni and Fe.

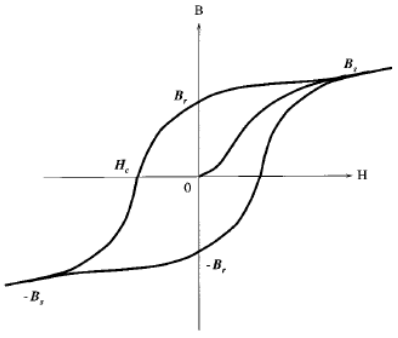

Figure 1. Hysteresis loop for a ferromagnets.

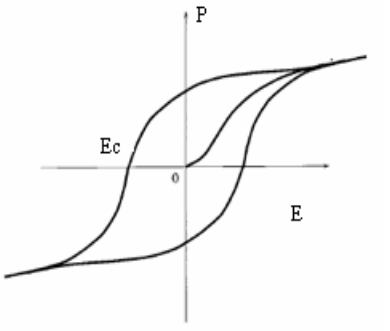

Figure 2. Hysteresis loop for a ferroelectrics

Ferroelectric materials display a spontaneous polarization (at E= 0) that can be oriented and switched by an electric field and, similarly to ferromagnets, ferroelectrics show P(E) hsyteresis loops (Figure 2). Contrary to ferromagnets, ferroelectrics need to be insulators. Examples of ferroelectrics are perovskite materials such as barium titanate or lead zirconate titanate (Figure 3). The electric polarization and the magnetization are influenced by temperature. They are largest at low temperatures and at high enough temperatures (above the so-called Curie temperature, T_c) they vanish as depicted on figure 3.

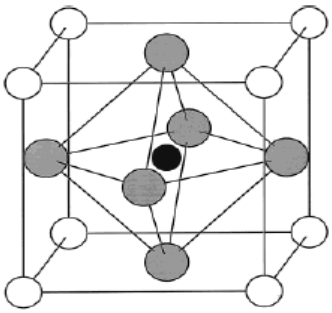

Figure 3. Cubic perovskite structure.

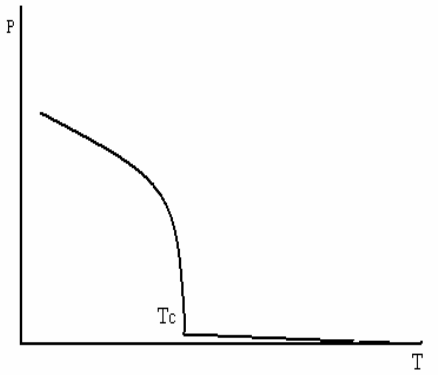

Figure 4. Polarization dependence on Temperature.

The origin of ferroelectricity is determined by balancing the two factors between the long-range Coulomb forces (which favour the ferroelectric state) and the short-range repulsions of the adjacent electron clouds (which favour the nonpolar cubic structure).

In 1992, Cohen and Krakauer[3] used the first principle calculation to learn about the ferroelectric in the best-known perovskite-structure materials such as $PbTiO_3$ and $BaTiO_3$ compounds. They pointed out that both crystals showed Ti 3d- O 2p hybridization, which is very important to stabilize the ferroelectric distortion. This tendency to hybridize requires d^0 ion states (as in Ti^{4+}). Unfortunately, d-orbital occupancy is required for the existing of magnetic moments and magnetic ordering[2], so it seems that ferroelectricity and magnetism exclude each other.

1.2. Magnetoelectric (ME) effects.

The coupling between magnetic and electric properties of a material gives rise to magneto-electric effects. The ME effects were very popular in the beginning of 19th century after their discovery by Curie and Röntgen. However, the progress understanding ME effects seems to have stopped since about 1970 because of the lack of materials and degrees of freedom to modify these effects.

The ME effects are determined by the transformation properties of the crystal in both space and time. These effects can be taken into account in the expansion of the free energy of a material, i.e:

$$F(\vec{E},\vec{H}) = F_0 - P_i^S E_i - M_i^S H_i - \tfrac{1}{2}\epsilon_0\epsilon_{ij}E_iE_j - \tfrac{1}{2}\mu_0\mu_{ij}H_iH_j - \alpha_{ij}E_iH_j$$

where P^S and M^S denote the components of the spontaneous polarization and magnetization and ε_{ij} and μ_{ij} are the electric and magnetic susceptibilities, respectively. (Note: Define also ε_o and μ_o) The tensor α_{ij} corresponds to the induction of polarization by a magnetic fields or of magnetization by an electric field and is designated as the linear ME effect[4]. The ME responses are limited under following relation:

$$\alpha^2_{ij} < \varepsilon_{ij}\,\mu_{jj} \text{ or } \alpha^2_{ij} < \chi^e_{ii}\,\chi^m_{jj}$$

From this expression it is then clear that in order to obtain the largest ME responses within one material, large dielectric constants and magnetic susceptibilities are important. Therefore, the most possible way to find ME effects is in the ferroelectrics and the ferromagnetics. The materials possessing these two properties so called multiferroics are the best candidates to show a strong ME effects. The ultimate goal is to obtain such a powerful ME effects that the electric polarization can be totally switched by magnetic field and the magnetization can be reversed by electric field as well, within a single phase.

1.3 Requirements of a multiferroic.

By definition, multiferroics can be defined as a material that simultaneously exhibits ferromagnetism and ferroelectricity coexisting within one phase. So multiferroics can show the largest ME effects, as discussed before. Nevertheless it does not mean that all ME materials are multiferroics. Unfortunately, these materials are quite hard to be found. The following limitations indicate why multiferroic materials are so rare.

A. Symmetries.

The existence of ferroelectricity can not be separated from the existence of a structural distortion from a high-symmetry phase. This distortion removes the center of symmetry and the atomic displacements produce a dipole per unit cell and, therefore, an spontaneous electrical polarization. There are 31 point groups that allow the spontaneous electric polarization, and 31 point groups of spontaneous magnetization as well[5]. Thirteen point groups (1, 2, 2′, *m*, *m* ′, 3, 3*m* ′, 4, 4*m*′*m*′, *m*′*m*2′, *m*′*m*′2′, 6, and 6*m*′*m*′) are found in both sets, allowing coexistence of these order parameters in the same phase. Since there are some materials included into these groups which do not display any relevant properties, this factor is apparently not responsible for the scarcity of ferromagnetic ferroelectric materials.

B. Chemistry "d^0-ness".

The common perovskite oxide materials possess a d^0 electron configuration on B cations to display ferroelectricity. When the d- electrons levels are partially occupied, then the tendency to make a distortion that removes the centre of symmetry is eliminated. On the other hand, we need d^n electrons to produce localized magnetic moments, otherwise it would not be magnetic ordering of any type, either ferro-, ferri- , or antiferromagnetic[5].

The following data shows comparison of small ionic radii cations of ferroelectric perovskite oxides with d^0 and d^n configuration electrons[7]:

d^0 cations		d^n cations	
Name	Radius (pm)	Name	Radius (pm)
Ti^{4+}	74.5	Mn^{3+} (d^4)	78.5
Nb^{5+}	78	Ti^{3+} (d^1)	81
Zr^{4+}	86	V^{4+} (d^1)	72

Typical B-site cations with occupied d-electrons do not have systematically larger radii than typical d^0 B-site cations. Therefore, it is assumed that the size of the B

cations is not really the important factor for the existence of ferrolectricity. The off-centre displacement of a small (B) cation in perovskites leads to the phase transition of ferroelectric materials. This can be achieved if the materials undergo the transition from high temperature phase to the low temperature phase. Nevertheless, the Jahn-Teller distortions become more important factor when it concerns some of the d-orbital occupancies. Unfortunately, this could reduce the driving force for the off-centre displacements and diminish the ferroelectric tendencies. One example that can be shown is in lanthanum manganite ($LaMnO_3$): The Mn^{3+} ion (with d^4 configuration) shows the elongated axes of the oxygen octahedral along to *c* axis. As result, there is an orbital ordering occurs simultaneously with the Jahn-Teller ordering. Hence, it is clear that the occupation of d electrons of small cations can reduce the ferroelectricity on perovskite oxides. Further, the first principle density functional theory calculations were conducted to observe the occurrence of ferroelectricity at one material. Therefore, the spins were removed artificially to determine whether ferroelectricity still existing or not. It turns out that the removal of magnetization did not affect the calculated phonon frequencies.

The above explanations clearly show that there is no strict rule to define multiferroic properties. However, there are competition factors between the absence and the occupancy of d orbitals of the multiferroics. These points might help to understand under which condition multiferroicity can appear in one material. For instance, rare-earth manganites show a strong coupling between magnetic and structural ordering parameters. The hexagonal of $YMnO_3$ crystal structure exhibit antiferromagnetic and ferroelectrics, whereas $BiMnO_3$ shows and ferromagnetic and ferroelectrics with a different trigonal structure even with the same general formula of perovskite oxides.

In principle, the fundamental requirement of multiferroicity is how to find a “non standar ferromagnet” that is not metallic. Since metals possesses the most probable way to show ferromagnetim such as Iron or Cobalt, in which they prohibit the spontaneous magnetization. In other case, insulator was needed to shows ferroelectricity when dipole moments are aligned into one preferential direction. Unfortunately it is very hard to find the ideal case where one material displays those properties into the same phase.

1.4. Some example of multiferroics structures.

Currently, there are four classes of multiferroic materials based on their crystallography forms: Perovskite, hexagonal, boracites and $BaMF_4$ structures. Most of the multiferroics have been known to possess these typical structures. In perovskites, the general formula is ABO_3 or $A_2B'B''O_6$[8]. Normally, multiferroic materials have a slightly deformed symmetry with the 3*m* point symmetry group instead of the ideal cubic symmetry *m*3*m*. One famous example is $BiFeO_3$, which is ferroelectric and antiferromagnetic. In particular, this material is interesting because of the high electric and magnetic ordering temperature about 1100 K and 650 K[9,10], respectively, which makes of $BiFeO_3$ the only known room temperature multiferroic compound.

The hexagonal structure can be built when a small cationic radii is placed in the centre of perovskites. For example, rare-earth manganites of $RMnO_3$ (where R = Sc, Y, In, Ho, Er, Tm, Yb, Lu) with their crystallographic point symmetry 6*mm*. The Boracite compounds have a chemical formula $M_3B_7O_{13}X$ (where M refers to Cr, Mn, Fe, Co, or Cu) and possess ferroelectric and weak ferromagnetic. Another example of multiferroics is $BaMF_4$ materials, where M can be metal elements such as Mg, Mn, Fe, Co, Ni, or Zn. These compounds have an orthorhombic structure with 2*mm* point symmetry at high temperatures.

1.5. Multiferroic thin films.

As said before, despite the remarkable applications that can be imagined for multiferroics, there are only few materials, either in the natural form or by synthetic routes, which possess these fascinating properties. Moreover, only a few multiferroic materials are found at room temperature, for example $BiFeO_3$. In bulk oxide system, several examples had been investigated and yet many discussions still arise among the scientist to explain the mechanism of multiferroicity, which is the first step to synthesize new better multiferroics. In particular, rare-earth manganites have been synthesized to investigate the correlation between the simple structure and their functionality, since this certain type has been predicted to have a large magnetoelectric coupling. Unfortunately many of these bulk manganites can be achieved only by high pressure, which is not easy. Therefore, people are trying new pathways using thin film preparation to be able to synthesize some of these compounds and to increase their performances.

2. Mechanism of Multiferroics

We have seen that 'standard' ferromagnetism and 'standard' ferroelectricity exclude each other. So in a multiferroic at least one of these two properties needs to have an unusual origin. In this section I would like to give an overview about the known mechanisms of multiferroicity. In addition, new proposed origins that people discuss in certain exotic manganites such as $TbMnO_3$, $DyMnO_3$ and $GdMnO_3$ with very strong magnetoelectric coupling will be discussed. These are related to the induction of polarization in spiral magnetic structures.

2.1. Some known mechanisms of multiferroicity.

Several mechanisms have been proposed to explain how multiferroicity originates in the different materials. The following description illustrates six different approaches with their own perspectives about how coexistence of ferromagnetism and ferroelectricity can occur.

1. *Paramagnetic doping.*
   Coexistence of ferroelectric and ferromagnetic order parameters can be established when a transition metal ion is being replaced partially by a paramagnetic ion. The solid solution $[PbFe_{2/3}W_{1/3}O_3]_{1-x}[PbMg_{0.5}W_{0.5}O_3]_x$[11] is the first systems in which magnetic and electric ordering have been found to coexist. The Mg and W ions are diamagnetic and cause the ferroelectricity, and the d^5 orbitals of Fe^{3+} ion are responsible for the magnetic ordering. Because of the mutually diluting properties, these systems possess low magnetic ordering temperatures.

2. *Lone-pair asymmetry.*
   The chemical compounds of $BiRO_3$ (where R = Fe, Mn, Cr) can exhibit multiferroicity when a lone pair of s^2 (Bismuth ion) hybridize with an empty p orbital of R-cation and causes a structural distortion which eventually introduces ferroelectricity. In Bi_2FeCrO_6 a spontaneous magnetization of $2\mu B$ and a spontaneous polarization of 80 μCcm^{-2} at room temperature is predicted[12]. Meanwhile, $BiMnO_3$ possesses saturated magnetic moment with the magnitude of 3.6 μB at 10 K. For $BiFeO_3$, bulk magnetization measurement shows 6.1 μCcm^{-2}.[13]

3. *Electrostatic and size effects.*
   The nature of ferroelectricity which is driven by the chemical mechanism have been described in previous section. Another different pathway was carried out especially in the hexagonal structure of $YMnO_3$. This crystal consists of non-connected layers of MnO_5 trigonal bypiramid corner-like linked by its in-plane oxygen ion (O_p). In addition, an apical oxygen ion (O_T) produces close-packed planes separated by a layered of Y^{3+} ions (depicted on the figure 5).

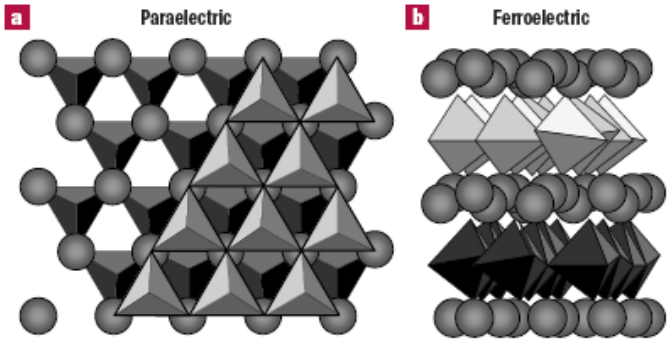

Figure 5 The crystal structure of $YMnO_3$ in the paraelectric and ferroelectric phases.The trigonal bipyramids depict MnO_5 polyhedra and the spheres represent Y ions. **a**,The stacking of two consecutive MnO_5 layers and the sandwiched Y layer,looking down the *c* axis in the paraelectric phase.**b**,A view of the ferroelectric phase from perpendicular to the *c* axis,showing the layered nature of $YMnO_3$. (ref:14)

There are two major atomic displacements in the crystal structure from the centrosymmetric $P6_3/mmc$ to the ferroelectric $P6_3cm$: First, a buckling of MnO_5 polyhedral structure which results shorter c axis. The second displacement is a vertical shift of the Y ions away from the high temperature mirror plane, while keeping the distance to OT constant[14]. As a result of this buckling phenomena, one of the two Y-O_P bond lengths is reduced, whereas the other bond length is enlarged. Consequently lead to a net electric polarization. This assymetric environment of the Y ions was recognized under neutron-powder-diffraction and X-ray diffraction studies.

Since Y^{3+} or Mn^{3+} have no lone pair of electrons and the Mn ions remains close to the centre of their oxygen cages, therefore the driving force for ferroelectricity in $YMnO_3$ is entirely caused by the electrostatic and size effects. This is derived from the long range dipole-dipole interaction and the oxygen rotated in such way to make huge Y-O_p off-centre displacements. Consequently, it produces an electrical polarization and a stable ferroelectric state occurrs in the $YMnO_3$ structure.

4. *Microscopy ME correlation.*
   Efremov, *et.al*[15] mentioned that besides the well-known site-centred and bond-centred charged ordering in doped manganites of the type $R_{1-x}Ca_xCaMnO_3$ (where E = La or Pr), there is one intermediate situation among them which can produce multiferroics.

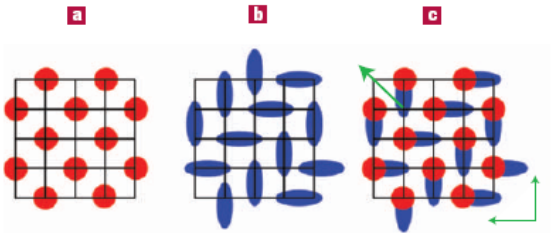

Figure 6. Three types of charge ordering. a, Site-centred charge order; b, bond centred and c, a ferroelectric intermediate state. Thin green arrows indicate the dipole moments of horizontal and vertical dimers, and the diagonal arrow is the total ferroelectric moment.(ref:15)

Charge ordering leads to a checkerboard ordering pattern (as shown in figure 6 (a)). This is known as Site-Centre Ordering (SCO). The other case may arise, when the charge ordering occurs on the bonds instead of in the sites, crystal as depicted on the 6(b) figure, the so called a Bond-Centre Ordering (BCO). For example, $Pr_{1-x}Ca_xMnO_3$ with x = 0.4 showed this particular mechanism. One situation where this intermediate mechanism could be found is in the doped Lanthanum-Calcium compounds at $x \geq 0.5$ and in the Pr-Ca system at x = 0.3. The asymmetry on this intermediate phase leads to an ordered dipole moment and consequently produces ferroelectricity. The schematic pictures above show the three different orderings.

2.2. Exotic Multiferroics: Magnetoelectric effect in inhomogeneous antiferromagnets

The case of ferromagnetic and ferroelectric couplings within one phase is very difficult to be found in reality: ferromagnets tend to be metals and ferroelectrics need to be insulators. At the moment, only one material possesses this idealized coupling which is $BiFeO_3$. Therefore, antiferromagnetic ferroelectrics, which are more common, are also counted among the multiferroics. This combination has shown the largest ME effects so far in single phase multiferroics with a 180^o switch of the electrical polarization by magnetic fields. Examples of these materials are the rare-earth manganites. They possess antiferromagnetic (AF) order with long wavelength modulation as compared to their chemical unit cell[16]. Rare-earth manganites RMnO$_3$ may be classified into those with hexagonal structure (where R = Ho,..,Lu) and those with orthorombically-distorted perovskite structures (where R= La, . . . ,Dy). Figure 7 shows the magnetic phase diagram for RMnO$_3$. The hexagonal RMnO$_3$ (such as YMnO$_3$ or LuMnO$_3$) show both, ferroelectric and antiferromagnetic order, but the $T_{FE} \approx 1000$ K and $T_N \approx 100$ K differ by an order of magnitude.[17] This is an obstacle faced by those manganites because it would not produce a feasible coupling between two order parameters. In contrast, RMnO$_3$ (with R = Gd,Tb, and Dy) possess comparable transition temperatures for the magnetic and the ferroelectric ordering, indicating that there might be direct coupling between them. For instance, the switching of the electric polarization could be performed by means of magnetic fields. The following section will describe shortly the differences and similarities between these materials in order to learn about their multiferroicity.

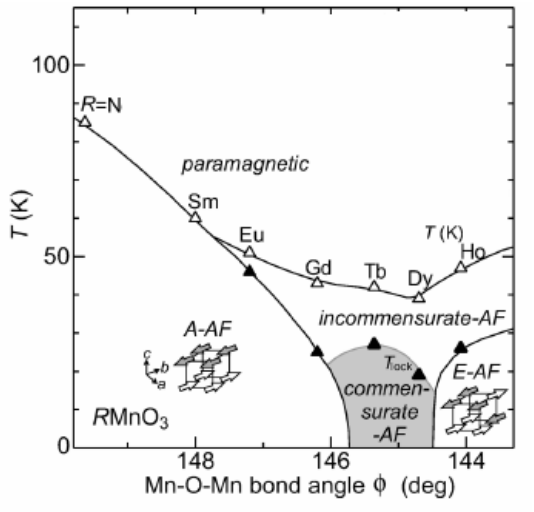

Figure 7. Magnetic phase diagram for RMnO$_3$ as a function of Mn-O-Mn bond angle Φ. Open and closed triangles denote the Ne´el and lock-in transition temperatures, respectively. (ref:18)

2.2.1 $TbMnO_3$.

Kimura *et.al* discovered that an orthorhombically perovskite manganites of $TbMnO_3$ exhibit ferroelectricity properties[19]. From the spin structure point of view, this material shows a different type of antiferromagnetic ordering (AF-order) compared with other multiferroic materials such as $BiMnO_3$ or $BiFeO_3$. The perovskite $TbMnO_3$ does not have any 6s lone pairs, which is apparently needed for producing a polar structure in magnetic ferroelectric perovskites as $BiMnO_3$ or $BiFeO_3$.

The spin frustration of Tb^{3+} moments leads to sinusoidal antiferromagnetic ordering of Mn^{3+} spins which orient along the b axis at low temperature (Figure 8). This phenomenon is followed by a magnetoelastically induced lattice modulation. Consequently, a spontaneous electrical polarization is induced by magnetic fields. The orange arrow is Mn magnetic moment below Neel Temperature (T_N). This temperature is a boundary for commensurate-incommensurate transition of material, where the magnetic modulation of wave vector K_s remains constant.

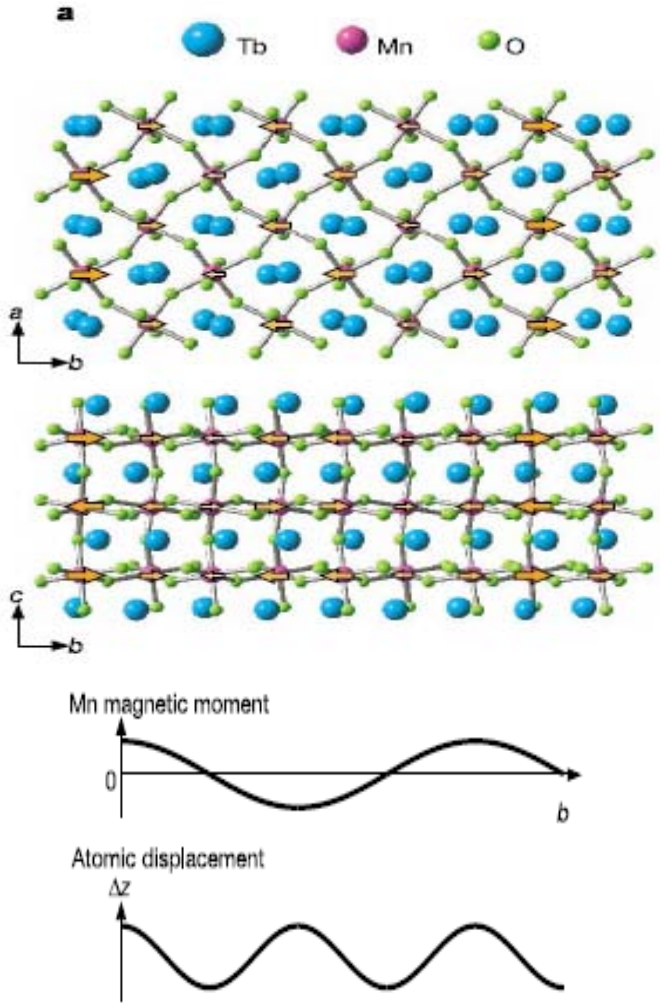

Figure 8. Appearance of ferroelectricity below a lock-in transition temperature in $TbMnO_3$. Rough sketches of crystal structure at room temperature (top) and spatial variation along the b axis of Mn magnetic moment and atomic displacement (Δz //c) below T_N (lower).(ref: 19)

After passing the temperature at 27 K, an incommensurate-commensurate transition of the magnetic system is observed. In accordance, there is a spatially varying electric dipole moment which associated with the magnetoelastic Mn^{3+} ion displacements. Another phase transition occurred at 7 K in which represent Tb^{3+} ordering. Indication of ME effects can be found when a spontaneous polarization at the c axis appeared and followed by the presence of static magnetic field along the b axis. After passing the critical field, a discontinuous change in magnetization was the sign for magnetic reorientation, either for Tb^{3+} and the Mn^{3+} spins. It followed by 90^0 rotation of the ferroelectric polarization from c to b. Hence, the spontaneous polarization can be controlled in such way under magnetic fields (Figure 9).

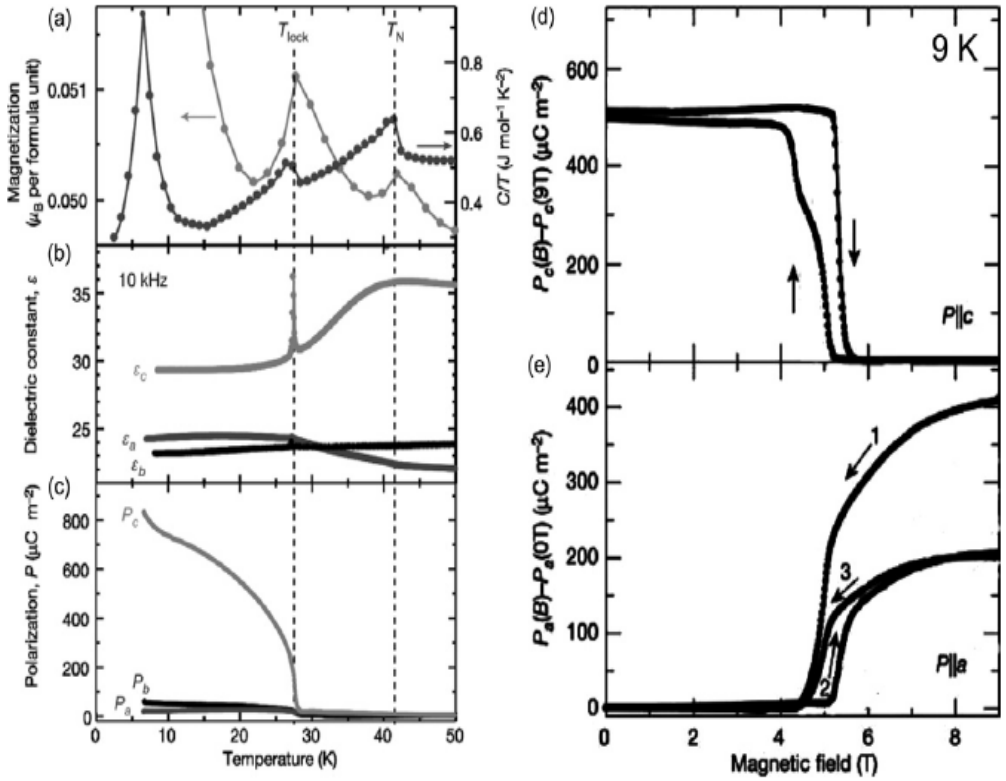

Figure 9. Magnetic control of ferroelectric polarization in $TbMnO_3$. (*a*) Temperature dependence of magnetization and specific heat divided by temperature. (*b*) Temperature dependence of dielectric constant at 10 kHz. (*c*) Temperature dependence of electric polarization along the principal axes. (*d*) and (*e*) Magnetic-field dependence of the ferroelectric polarizations along the *c* and *a* axes. At 5 T the ferroelectric polarization is flipped by the magnetic field applied along the *b*
Axis (ref:16)

2.2.2 $DyMnO_3$.

The magnetic, structural, and ferroelectric properties of an orthorhombic crystal of $DyMnO_3$ are similar to those of $TbMnO_3$. This material also shows an incommensurate crystallographic superstructure below T_N(Mn) at 39 K corresponding to a sinusoidal AF ordering of the Mn moments[20]. The magnetic-field effect on the ferroelectric properties in $DyMnO_3$ has been studied extensively by group of Kimura et al. The magnetoelectric phase diagrams of $DyMnO_3$ for the directions of *H* along *a*, *b*, and *c* axes were shown in figure 10. The important features are almost the same as in the $TbMnO_3$ profile. Namely, *H* changes the ferroelectric polarization vectors from *c* to *a* axis. However, the

magnitude of H needed for the transition is smaller in $DyMnO_3$ than that in $TbMnO_3$. By analogy with $TbMnO_3$, the superstructure in $DyMnO_3$ can also be described by a magnetoelastically induced lattice modulation. At $T_{lock}(=T_C)$, ferroelectric order develops with a spontaneous polarization along the b axis. [30] Anomalies in the capacitance and P have also been observed around T_N(Dy)10K.[21]

Observation of hysteresis loops in the P–E curves is conducted to measure the degree of ferroelectricity. Hence, it is interesting to compare the P–E curves in magnetic fields below and above magnetic-field-induced polarization flop. Figure 11 shows the 4.2 K P–E curves obtained at 0 and 6 T. Here, magnetic fields were applied along the b axis while electric fields were parallel to a axis. No hysteresis loop was observed at 0 T (red line). Meanwhile, a clear hysteresis loop of ferroelectrics was observed in a magnetic field of 6 T. The results revealed that the ferroelectric polarization vector switch from the c to a axis by applying a magnetic field H_b.

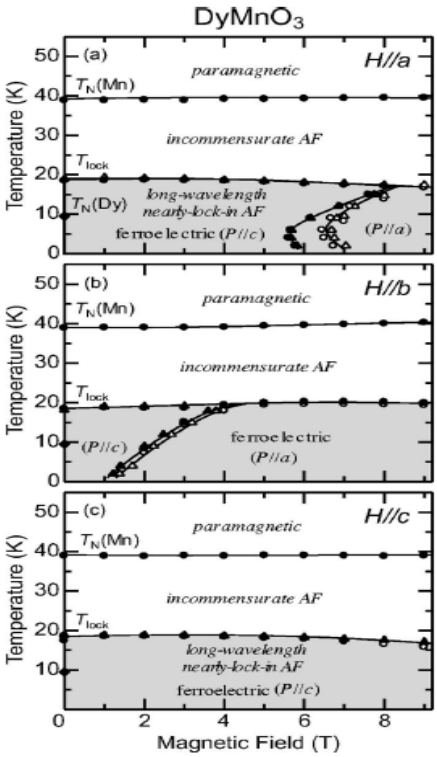

Figure 10. Magnetoelectric phase diagram of $DyMnO_3$ with magnetic field along the a (a), b (b), and c (c) axes. Circles, triangles, and diamonds represent the data obtained by measurements of dielectric constant, pyroelectric or (magneto-electric) current, and magnetization, respectively. Gray regions indicate ferroelectric phases. (ref: 20)

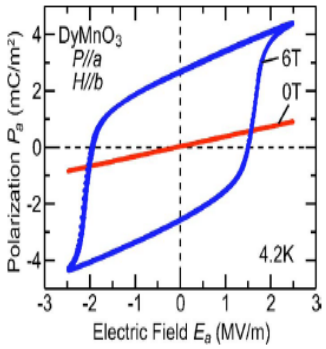

Figure 11. P–E curves obtained at magnetic fields of 0 T (red) and 6 T (blue) for a $DyMnO_3$ crystal. The measurements were done at 4.2 K and 100 Hz. Magnetic and electric fields are applied along the b and a axes, respectively. (ref: 20)

2.2.3 $GdMnO_3$.

The orthorhombic crystal structure of $GdMnO_3$ also exhibits a lattice modulation characterized by the propagation vector $(0,k_l,0)$ below T_N(Mn) ≈43 K.[20] The lattice modulation between T_N (Mn) and T_{lock} suggests there may be a modulated spin structures observed on those ranges. However, the disappearance of the lattice modulation below T_{lock} implies that the long wavelength modulated spin structure is transformed into another structure in $GdMnO_3$. It assumed that the sinusoidal AF structure ($\sim 0.2 < k_{Mn} < \sim 0.24$) above T_{lock} changes into A-type AF order ($k_{Mn}= 0$) below T_{lock}, motivated by the known magnetic phase diagram for $RMnO_3$.[21] In addition, a recent magnetization study of $GdMnO_3$ also indicates the existence of A-type AF order on Mn sites below T_{lock}.[21] $GdMnO_3$ may not be ferroelectric in the absence of a nonzero wave vector lattice modulation below T_{lock}. The location

of $GdMnO_3$ in the magnetic phase diagram is in the immediate vicinity of the phase boundary between *A*-type and long-wavelength AF phases. This make the ferroelectric properties of this particular system quite complicated.

In order to study the coupling of the various phase boundaries to the lattice degrees of freedom of $GdMnO_3$, Baier and his coworkers[22] conducted a various high resolution measurements of thermal expansion and magnetostriction. It turns out that anomalies appeared at all transitions. For instance, a transition of incommensurate antiferromagnetic order (ICAFM) to a canted A-type antiferromagnetic Ordering (cAFM). A downbending of the ICAFM-to-cAFM phase boundary is observed in low magnetic fields and there is an evidence for a coexistence of both phases in this low field range. Unlike $TbMnO_3$ and $DyMnO_3$, the ground state of $GdMnO_3$ is not ferroelectric in the absence of magnetic fields. However, ferroelectric order can be induced by the application of a rather low magnetic field ($\approx$<1 T) along the *b* axis. The ferroelectric phase with *P* along *a* axis induced by H_b is identical with those in $TbMnO_3$ and $DyMnO_3$.

In summary, the above manganites shows that a sinusoidal spins behavior driven by magnetic fields is induced the lattice modulations of the crystal. Further, these interactions will produce an electric polarization in the rare-earth manganites. The Neel and Lock-in transition temperatures of those rare-earth manganites show a comparable result which tabulated in the following. ($T_{lock\text{-}in}$ is close to T_C in this case)

Rare-earth Manganites	Lock-in transition Temperature	Néel Temperature
$TbMnO_3$	27 K	41 K
$GdMnO_3$	23 K	43 K
$DyMnO_3$	18 K	39 K

For comparison, the table below shows other perovskite multiferroics, such as $BiFeO_3$, $BiMnO_3$ or $YMnO_3$.

Rare-earth Manganites	FE Curie Temperature	Néel Temperature (except $BiMnO_3$ is FM T_C)
$BiFeO_3$	1083 K	653 K (ref:23)
$BiMnO_3$	750 K	105 K (ref:23)
$YMnO_3$	900 K	70 K (ref:14)

It is then clear that the temperature gap of the above perovskite oxides is too wide, which makes magnetoelectric couplings are hardly to achieve on that particular group. Meanwhile, the rare-earth manganites has shown a small gap between $T_{lock\text{-}in}$ and T_N and act as a promising multiferroic materials. However, they only exist well below room temperature.

2.2.4. Spiral Magnets.

These results have inspired M. Mostovoy to explain multiferroicity in magnetic systems from a phenomenological point of view, by using symmetry arguments.[25] Rare-earth manganites such as $TbMnO_3$ has been shown to have an electric

polarization in magnetically ordered states. In particular, to study the anomalies in dielectric constant at magnetic transitions and electric polarization flops in magnetic fields. A simple expression was produced for the electric polarization that is induced by an spin-density-wave (SDW) of the form.

$$\mathbf{M} = M_1\mathbf{e}_1 \cos\mathbf{Q}\cdot\mathbf{x} + M_2\mathbf{e}_2 \sin\mathbf{Q}\cdot\mathbf{x} + M_3\mathbf{e}_3,$$

Where the unit vectors e_i, i =1; 2; 3 form an orthogonal basis. If only M_1 or M_2 is nonzero, this equation describes a sinusoidal wave [see Figure 12(a)]. In other case, for M_1 *and* M_2 different than 0, it describes an (elliptical) helix with the spin rotation axis $\mathbf{e}_3$ (if alsoM_3 = 0, the helix is conical). Then the average polarization is transverse both to $\mathbf{e}_3$ and Q [see Figure. 12(b)], and also it is independent to M_3 as depicted on the following mathematical formula:

$$\bar{\mathbf{P}} = \frac{1}{V}\int d^3x\mathbf{P} = \gamma\chi_e M_1 M_2[\mathbf{e}_3 \times \mathbf{Q}].$$

It turns out that there is no observation of average polarization when it is induced by a sinusoidal (SDW) states, as the inversion symmetry at the sites where the magnetization reaches maximum or minimum [e.g., on the dashed line in Fig. 12(a)] remains unbroken[25]. This approach can also explain the suppression and change of direction of the polarization observed in the experiments when applying a magnetic field along different direction. If the weak fields are applied to these materials, the spins will rotate in the easy *xy* plane, and as a result the spin rotation axis $\mathbf{e}_3$ is parallel to the "hard" axis. Meanwhile in the strong magnetic fields environment, the spins perform a canonical helix with $\mathbf{e}_3$ || **H**. This spin flop will reduce the electric polarization if H is along x[see Fig. 13(a)]. On the other hand, magnetic field in the *y* direction will favor the rotation of spins in the *xz* plane, in which case **P** || **z** [see Fig. 11(b)].

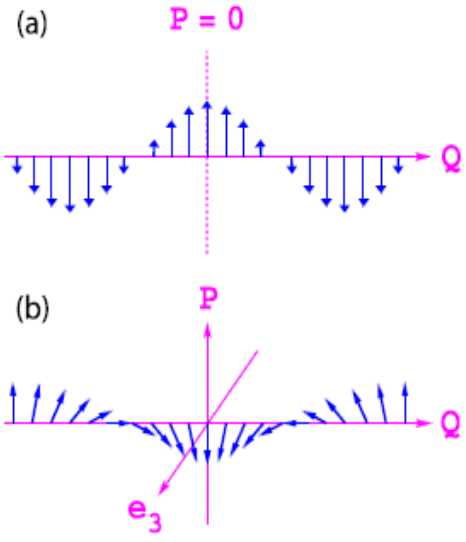

Figure 12. Sinusoidal SDW (a) does not induce Preparation of thin films oxide gives electric a uniform electric polarization; for a helicoidal SDW the xy (b) **P** is orthogonal both to the spin rotation direction and the wave vector **Q**. polarization.

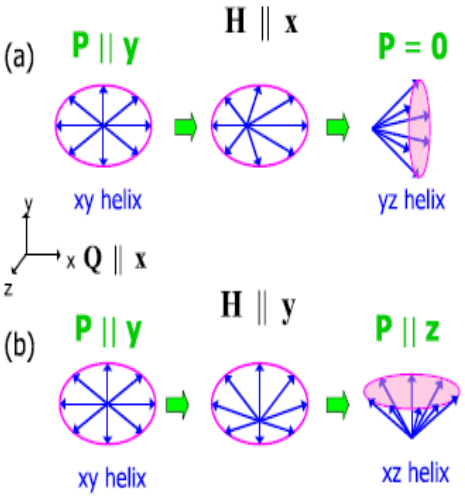

Figure 13. Magnetic field behavior of polarizations. In zero field spins rotate in plane and P || y . Magnetic in the *x* axis $\mathbf{e}_3$ suppresses the while *Hy* orients **P** in the *z* direction.

3. Thin Film Multiferrroics

Preparation of thin films oxide gives a controlled way of synthesizing multiferroic materials. A smooth surface of thin films can be achieved by Pulsed Laser Deposition (PLD) technique. In addition, Reflection High Energy Electron Diffraction (RHEED) was assembled into the PLD to monitor the growth of thin films especially for multiferroics. There are two distinguished work progress of thin films that had been evolved, i.e., single-layer compounds and multicompounds which include the superlattice and also the nanocomposites materials. In this paper, I will focus on the single layer compounds and gives an overview about how they can contribute to enhance the magnetoelectric coupling by means of strain effects. In the last section, several examples of multiferroic thin films were introduced to compare the magnetoelectric coupling with their respective bulk oxide systems.

3.1. Pulsed Laser Deposition & *in situ* monitoring Techniques

Pulsed-laser deposition (PLD) has obtained a great deal of attention in the past few years for its ease of use and success in depositing materials of complex stoichiometry. The PLD method of thin film growth involves evaporation of a solid target in an Ultra High Vacuum chamber by means of short and high-energy laser pulses. Many materials that are normally difficult to deposit by other methods, especially multi-element oxides, have been successfully deposited by PLD. The main advantage of PLD derives from the laser material removal mechanism, where the laser-induced expulsion produces a plume of material with the stoichiometry similar to the target. It is generally easier to obtain the desired film stoichiometry for multi-element materials using PLD than with other deposition technologies. Thus the thin film formation process in PLD consists of the following four steps: Laser radiation interaction with the target, dynamic processes of the ablation materials, deposition of the ablation materials with the substrates, and nucleation and growth of a thin film on the substrate surface.

One way to synthesize the growth of thin film in controllable manner is by using PLD, which combine with the Reflection High Energy Electron Diffraction (RHEED). These instruments are suitable for *in situ* monitoring technique to check the development of thin films during deposition process. RHEED basically has two main components, which are an electron gun and fluorescent screen to produce a picture which contains the structure and/or morphology of a crystal surface. The consumption of energy is between 5-100keV and it also employ lower impact angles ($<5^0$) compare to LEED (Low Energy Electron Diffraction). The higher energy of impacted electron in the sample may increase the resolution of image, and the lower angles enhance the electrons just pass a few atomic layers into the crystal. This make RHEED pictures only represent the structure of the surface instead of the whole feature of crystal. However, the preparation of multiferroic thin films encounter barrier since it hampered by a relatively high oxygen pressure atmosphere. In order to overcome this problem, The group of Rijnders, *et.al*[26] has been successfully modified RHEED by using a two-stage differential pumping systems. Consequently, the deposition pressure of was powered up to 50 Pa for complex oxides.

3.2. Some Examples of Multiferroic thin films.

The following thin films are described in the spirit of understanding the strain effects on each particular oxide systems Then the structural behavior are observed when it changes from one unique crystal structure to the other forms. In addition, the symmetry aspect also considered to see the comparison with bulk systems.

3.2.1. $BiFeO_3$ Thin Film.

Palkar *et.al*[27] reported that the $BiFeO_3$ film was made on silicon and $SrTiO_3$ substrate using a pulsed laser deposition technique. From the point of view thin film, the structure has a different crystal structure compared to bulk situation. Normally, $BiFeO_3$ has a rhombohedral in bulk, whereas several persons such as Yun *et, al* found a tetragonal structure (space group P4*mm*). This indicates that the substrate-induced strain has an influence on the crystal structures. Another factor must take into account is oxygen pressure during the deposition process. The c/a ratio is proportional with the amount of oxygen pressure applied during the preparation of thin film.

The measurement of ferroelectric hysteresis loop observed for such film is one the most interesting result especially in the thin film forms (Figure 14). In the case of $SrTiO_3$ substrate, $BiMnO_3$ thin film has a spontaneous polarization (50-60 μC cm^{-2}). Another example, in Silicon substrate, a spontaneous polarization of the 200 nm thick films was observed at 45 μC cm^{-2}. If using a single crystal $SrTiO_3$ as substrate along two orientation (100) and (111) direction. The results are 55 μC cm^{-2} and 95 μC cm^{-2} respectively[27]. The latter has a higher magnitude probably due to strong strained than previous one. The stress induced by the substrate which strongly affected to the ferroelectric properties of thin $BiFeO_3$ films. Moreover, the easy axis of spontaneous polarization lies to (111) for several orientation thin films. In fact, this was confirmed by the thickness-dependent magnetism compared to the bulk. The following figure 15 shows the sample of thickness dependence of 200 nm thick of $BiFeO_3$ which grown on top of $SrTiO_3$ substrates.

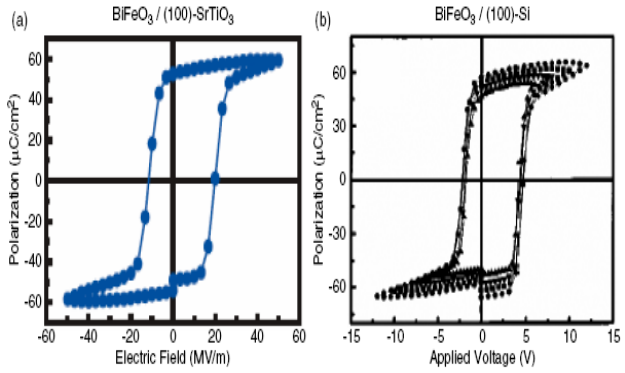

Figure 14. Ferroelectric hysteresis loop for $BiFeO_3$ measured at a frequency of 15 kHz on (a) (100) $SrTiO_3$ substrate and (b) (100) Si substrates.

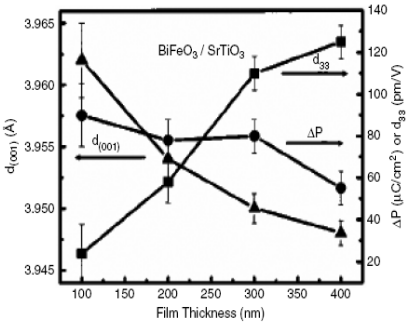

Figure 15. Thickness dependence of the out- of-plane (d_{001}), polarization (ΔP) and piezoelectric coefficient (d_{33}) for 200 nm thick $BiFeO_3$ films grown on Si substrates with $SrTiO_3$ as a template layer.

The change of polarization is relatively small, whereas for a piezoelectric constant d_{33} exhibit huge increase for 30 pm V^{-1} (thickness 100 nm), meanwhile for 120 pm V^{-1} (thickness 400 nm). Ferromagnetic behavior also concerned in thin film phase. It shows a weak ferromagnetic hysteresis loop at room temperature, in addition the remnant magnetization is twice compared to the the bulk system.

Ramesh, *et.al* had been successfully produced the thin film of $BiFeO_3$ by pulsed laser deposition method[13]. However, the film has a different monoclinic crystal structure compared with the previous result. $BiFeO_3$ (BFO) thin films was grown in the various thickness started from 50 to 500 nm onto single crystal $SrTiO_3$ (100 direction) (STO) substrates. In order to maintain heteroepitaxially growth process, therefore a $SrRuO_3$ (SRO) was applied as an oxide electrode. The physical properties of $BiFeO_3$ thin film were studied to understand the constrained crystallographic state in the BFO layer. For instance, polarization hysteresis and pulsed polarization measurements had been conducted to reveal the ferroelectric properties. 200-nm-thick $BiFeO_3$ film were measured to have remanent polarization (P_r, 50 to 60 μC/cm^2) which is much bigger value than the highest reported value of 6.1 μC/cm^2 from bulk BFO.

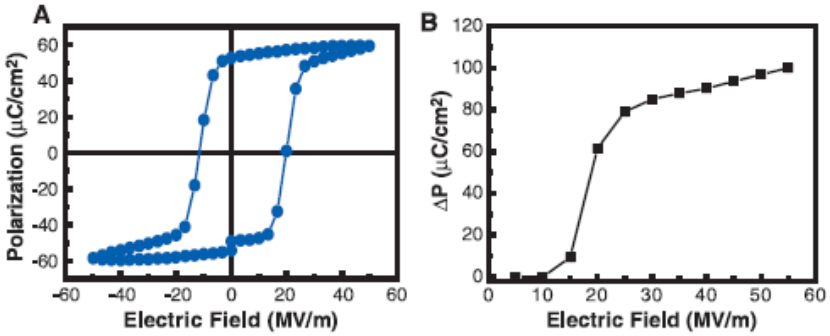

Figure 16. (**A**) Aferroelectric hysteresis loop measured at a frequency of 15 kHz, which shows that the film is ferroelectric with *P*r ~ 55 μC/cm2. (**B**) Pulsed polarization Δ*P* versus electric field measured with electrical pulses of 10μs width.(ref:13)

Magnetic response of 70-nm-thick film BFO shows the saturation magnetization at ~150 electromagnetic unit (emu)/cm^3(Figure 17). In addition, other information can be derived from the observation; there is a thickness dependence of the magnetization points to the effect of the mismatch strain on the magnetic response

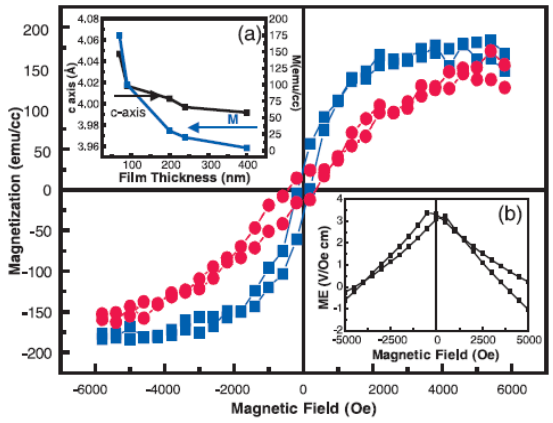

Figure 17. Magnetic hysteresis loops measured by vibrating sample magnetometry for a 70-nm-thick BFO film, showing an appreciable saturation magnetization of 150 emu/cm^3 and a coercive field of 200 Oe. The in-plane loop is shown in blue, and the out-of-plane loop is in red.

The observation of a thickness dependence of the magnetization shows that the effect of the mismatch strained on the magnetic response. Further, the coupling between two order parameter lead to magnetoelectric (ME) effect. It indicates on the inset (b) figure above that the *dE*/*dH* coefficient as high as 3 V/cmOe at zero fields.

As summary, $BiFeO_3$ thin film exhibit the large spontaneous polarization due to direct consequences of the heteroepitaxial stabilization of a monoclinic phase. This film also has a high enhancement of magnetization compared with the bulk system.

3.2.2. $BiCrO_3$ thin film.

$BiCrO_3$ is another great posssibillity to create a multiferroic thin film. Unfortunately, due to the necessity of high pressure system (40 kbar) synthesis, the ferromagnetic and ferroelectric properties have not been unambiguously established.[28] The group of Murakami et.al[29] had been successfully grown an epitaxial single phase $BiCrO_3$ thin film under pulsed laser deposition with various substrate $LaAlO_3$ (LAO)(001), $SrTiO_3$ (STO) (001), and $NdGaO_3$ (NGO) (110). Preparation method were initiated by ablated the stoichiometric of $BiCrO_3$ target with KrF excimer laser (λ=248 nm) with oxygen pressure and the substrate temperature during deposition were varied in the ranges of 01-50 mTorr and 550-750^0 C, respectively. In addition the deposition rate was operated 5nm/min. The characterization of thin film conducted by several methods: Transmission Electron Microscopy (TEM), Scanning X-ray microdiffraction, superconducting quantum interference device (SQUID) to examine the magnetic characterization. In addition, piezoelectric force microscopy and microwave microscopy were used to analyze the ferroelectricity of $BiCrO_3$ thin films at room temperature.

The magnetization against temperatures were depicted bellow on LAO (001) substrate for zero field cooled (open squares) and field cooled (solid circles) with a 1000 Oe magnetic field applied in the in-plane direction. The ferromagnetic transition was carried out at around 120 K. In addition, the hysteresis loop of sample at 5 K observed as depicted on figure 18. Both result are in agreement with the report by Niitaka et,al. The magnetic moment of the film is 0.05 μ_B/Cr. The observation is consistent with the prediction that Cr spins are antiferromagnetically coupled and the canting of the spins obtained the weak ferromagnetic below 120 K.

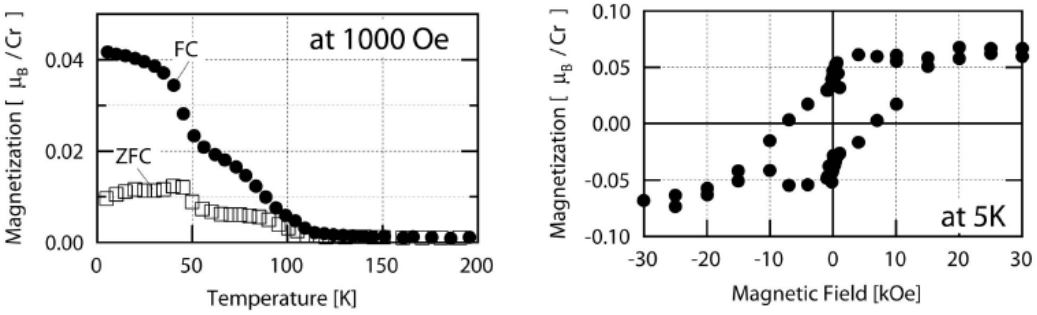

Figure 18. Temperature dependent magnetization curves (a) and a magnetic hysteresis curve (5 K), (b)of a $BiCrO_3$ thin film fabricated on a $LaAlO_3$\(001) substrate.

Figure 19 plots the nonlinear dielectric signal as a function of dc voltage bias applied together with the ac voltage. The nonlinear signal is proportional to $d\varepsilon/dV$, where ε is the dielectric constant and V is the ac voltage. The dc voltage of ±5.5 V is apparently not high enough to observe the expected saturation behavior, but a small hysteresis is observed. So far, the magnetoelectric coupling behavior of related films is currently under investigation.

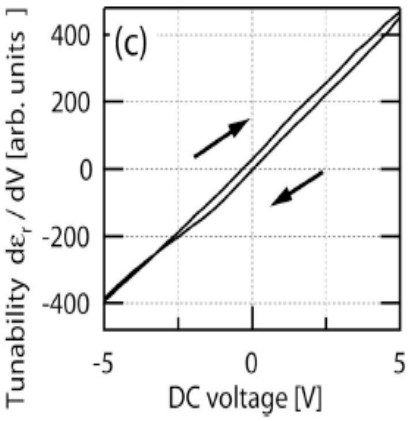

Figure 19. Nonlinear dielectric signal as a function of dc voltage which measured by the lock-in amplifier.

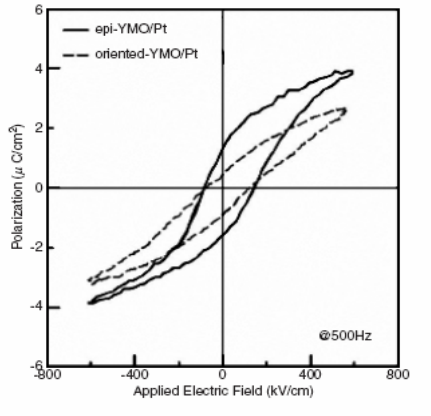

Figure 20. Polarization–electric field (*P–E*) dependence between the epitaxial and the oriented $YMnO_3$.

3.2.3. $YMnO_3$ thin film.

These materials consist of two stable crystallographic structures: orthorhombic and hexagonal. The latter structure can be synthesized through molecular beam epitaxy, laser ablation, or sputtering. In addition, many substrates can be implemented to produce $YMnO_3$ thin films. The fabrication of $YMnO_3$ hexagonal structures are strongly dependence on the orientation of substrates. For instance, the films with (111) MgO and (0001) ZnO:Al/(0001) sapphire possess an epitaxial forms. Meanwhile the preparation under preferential direction of substrate on (111) Pt/(111) MgO will produce polycrystalline form.[23] The evidence of ferroelectric materials can be seen on the P-E curve (Figure 20) which shows a hysteresis loop. Nevertheless, there is a saturated condition that occurs on the epitaxial form at a spontaneous polarization 4.0μCcm^{-2} and remnant polarization of 1.7 μC cm^{-2}, and coercive field at 80kV cm^{-1}. If compared to the oriented direction, the results are: spontaneous and remnant polarization, 2.8 μC cm^{-2} and 0.7 μC cm^{-2}. In addition, the coercive field has been detected with the magnitude 70 kV cm^{-1}.

The group of Posadas, et.al had been successfully grown $YMnO_3$ multiferroic thin film on GaN substrate. Both materials are known to be hexagonal structure with a nominal lattice mismatch of 4%[30]. However, the X-ray diffraction reveals an unexpected 30° rotation between the unit cells of $YMnO_3$ and GaN that results in a much larger lattice mismatch (10%) compared to the unrotated case. The first principles calculations show that the bonding energy was obtained from the atomic rotated arrangements compensates the increase in strain energy due to the larger lattice mismatch. These calculations show that large energy stabilization can be obtained from bonding at the interface. It must overcome the elastic energy cost to result in the 30° rotation. The observed epitaxial relationship between

$YMnO_3$ and GaN show that there is thickness dependence appeared on this construction.

Ferroelectric characteristics of the $YMnO_3$ films were measured using standard electrical measurements. It turns out that the ferroelectric hysteresis showed coercive field ~50 kV/cm and a remnant polarization of ~2 μC/cm^2 (Figure 21). Meanwhile, the magnetic properties were determined using SQUID device magnetometer under an applied field of 0.1 T. As result, the magnetization shows Curie-Weiss behavior at high temperatures with a steep increase in the field-cooled measurement at 45 K, indicating the Neél temperature of the $YMnO_3$ thin films.

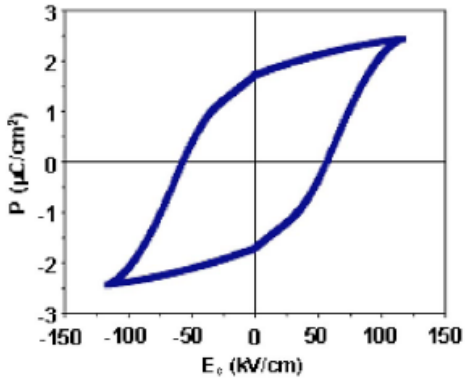

Figure 21. Ferroelectric hysteresis loop of $YMnO_3$ with orientational a coercive field of 50 kV/cm and a remnant polarization

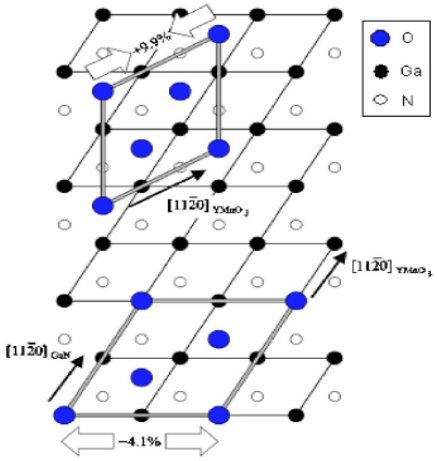

Figure 22. Schematic of the in-plane relationship between the GaN substrate and the of 2 μC/cm^2 $YMnO_3$ film for aligned unit cells with 4.1% tensile strain (bottom) and unit cells with a 30° offset with 9.9% compressive strain (top)

The relative energies formation of $YMnO_3$ thin films are estimated from the first principles computations. In order to understand the orientation between the unrotated interface and the 30° rotated interface. First, the elastic strain energy were gained from strained bulk $YMnO_3$, with the measured strains imposed in the plane, relative to theoretical unstrained bulk $YMnO_3$. It turns out that the lattice strain energy of 30^0 rotations has a larger result compare to the unrotated situation.

The bonding prediction between $YMnO_3$ and GaN is simulated in figure 22. Each of $YMnO_3$ unit surface contains three apical oxygens, they must be bond to the GaN surface. In addition, There are four different types of bonding sites on the GaN (0001) surface: the hcp site (on top of subsurface N), the fcc site (on top of the threefold cavity), the on-top site (on top of surface Ga), and the bridge site (in between two Ga surface atoms). In the unrotated case, these three oxygens will bond to GaN in such way only one oxygen positioned itself on fcc site, one on an on-top site, and the last one on an hcp site. These results in an average energy obtain 5.16 eV per $YMnO_3$ formula unit. The 30° rotated case shows energy gain of 0.15 eV per $YMnO_3$ formula unit (or 0.45 eV per $YMnO_3$ unit cell) over the aligned case, making the 30° rotated case more energetically favorable, which is in agreement to the experimental observations.

4. Summary and conclusions

Multiferroicity offers a chance to understand and use the unusual behavior of magnetism and ferroelectricity coexisting in one phase. Unfortunately these materials are difficult to be found in nature or to obtain by synthetic routes. Several oxides in the perovskite family, such as $BiMnO_3$ and $YMnO_3$ or even $BiFeO_3$, are examined as candidates to show multiferroic behavior. It turns out that they display promising high ferroelectric (FE) Curie temperatures for their use in room temperature applications. However, these materials are mostly antiferromagnets (with no macroscopic magnetization), which limits their applicability, and exhibit a huge gap between the FE Curie temperature (T_C) and the Néel temperature (T_N), which makes the coupling between the two order parameters unlikely. People are trying to find new multiferroic materials with larger magnetoelectric (ME) couplings. The rare-earth manganites ($RMnO_3$), showing low T_C and T_N temperatures, have been pointed out as an interesting alternative.

Within the rare-earth manganites, in the orthorhombic structures with small ionic radius (R = Gd, Tb, and Dy), there is a competition between the ferromagnetic interaction between nearest-neighboring Mn sites and the antiferromagnetic (AF) ordering of next-nearest-neighboring sites, which gives rises to ferroelectricity via magnetoelastically induced lattice modulations. This produces a larger magnetoelectric coupling. However T_N and T_C are too low to be useful for room temperature applications.

Other possible phases of multiferroics have been pursued. In order to seek better performances, smooth thin films of multiferroics have been shown to possess a larger polarization and high magnetolectric couplings. Several examples such as $BiFeO_3$, $BiCrO_3$ and $YMnO_3$ thin films, which show a large spontaneous polarization, in some cases even larger than their respective bulk systems. In addition, a measurable macroscopic magnetization has been reported in some of these films. For instance, in the case of $BiFeO_3$, which in bulk shows a rhombohedrally distorted perovskite structure, in thin film form, the structure is sensitive to substrate-induced strains and to the substrate orientation. Because of this, the observed remanent polarization (P_r, 50 to 60 $\mu C/cm^2$) of 200 nm-thick films of $BiFeO_3$ is much bigger value than the highest reported value of 6.1 $\mu C/cm^2$ in bulk.

As mentioned above, the orientation is a very important factor in the growth of thin films in order to increase their spontaneous polarization, since the application of a field along the easy axis will enhance the polarization of a particular thin film. For example, $BiFeO_3$ thin films were grown on top of $SrTiO_3$ substrates along two different orientations: the (100) and (111) directions. The resulting polarizations were 55 $\mu C\ cm^{-2}$ and 95 $\mu C\ cm^{-2}$ respectively. The latter has a higher magnitude probably due to a stronger strain value compared to the former one. Another important result on the thin film research is the thickness dependence of the magnetization, due to effect of mismatch strain on the magnetic interactions.

In addition, the epitaxial forms have a better quality than the polycrystalline oriented forms in the performance of thin films. This can be concluded after several investigations which clearly show that the higher magnitude of either the spontaneous polarization or magnetization is recorded on epitaxial thin films. Multiferroic thin films have shown a remarkable improvement of the magnitude of the order parameters with respect to their respective bulk counterparts. However, they still could not produce an ideal example of multiferroic that can be used in a room temperature device using both order parameters. Nevertheless, these steps have built the foundation to understand the unique behavior of multiferroics especially in the manganites family.

5. Prospects.

Multiferroic thin films remain as promising candidates in the research of magneto-electric materials. However, the availability of materials which possess high magnetoelectric couplings at room temperature is still unsolved. Therefore, new experimental work and investigation from the theoretical point of view become important issues on multiferroic thin film research. Further improvements to grow multiferroic thin films on other substrates, such as semiconductors, are currently being investigated. These steps will enhance the development on multifunctional devices that couple the rare-earth manganites with the wide band gap semiconductors. Moreover, they also offer the study of the origin of multiferroicity and the interaction between ferroelectricity and magnetism in these relevant materials. Another up-to-date topic that has been recently introduced is the work on nanocomposites. The heterostructure arrangements exhibit a combination of alternating layers of ferroelectric phase (for instance, perovskite) and ferromagnetic phase (for instance, spinel-structure). These structures are promising for application in multi-state storage devices. At the end, multiferroic thin film research is greatly influenced by the intrinsic difficulty to find robust ferroelectric and ferromagnetic order parameters coexisting within one phase.

6. Acknowledgements

I would like to thank Beatriz Noheda for supervising me during this paper project.

7. References

[1] Ascher, E.; Rieder, H.; Schmid, H.; Stössel, H. *J. Appl. Phys.*, **37**, 1404 (1966).
[2] Wood, V. E.; Austin, A. E. In *Magnetoelectric Interaction Phenomena in Crystals*; Freeman, A. J., Schmid, H., Eds.; Gordon and Breach: Newark, NJ, (1975).
[3] Cohen, R. E.; Krakauer, H. *Ferroelectrics* **136**, 95 (1992).
[4] Fiebig M, *J. Phys. D: Appl. Phys*. **38.**123 (2005).
[5] Schmid, H. *Ferroelectrics* **162**, 317 (1994).
[6] Hill. N. *Phys. Chem. B*. **104**, 6694 (2000).
[7] Shannon, R. D. *Acta Crystallogr.***A32**, 751 (1976).
[8] Smolenskii G A and Chupis I E ,*Sov. Phys.—Usp.* **25**, 475 (1982).
[9] Kubel F and Schmid H *Acta Crystallogr.* B **46**, 698 (1990).

[10] Kizelev S V, Ozerov R P and Zhdanov G S *Sov. Phys.—Dokl.***145**, 1255 (1962).
[11] Srinivasan G, Hayes R and Bichurin M I *Solid State Commun.* **128**, 261 (2003).
[12] Khomskii D I *Bull. Am. Phys. Soc.* **21**,002 (2001).
[13] Wang. J, *Science*, **299**, 1719 (2003).
[14] Van Aken, et.al, *Nature Material*, **3**, 164 (2004).
[15] Efremov D V, et.al. *Nature Material.*. **3**, 853 (2004).
[16] D. Higashiyama, et. al, *Phys. Rev. B* **70**, 174405 (2004).
[17] Fiebig. M, et.al , *Nature*, **419**, 818 (2002).
[18] Kimura. T, et.al, *Phys. Rev Lett.* , **92**, 257201-1 (2004).
[19] Kimura T, et.al, *Nature* **426**, 55 (2003).
[20] Kimura, T et.al, *Phys. Rev. B* **68**, 060403(R) (2003).
[21] J. Hemberger, et.al, *Phys. Rev. B* **70**, 024414 (2004).
[22] Baier J, et.al, Phys. Rev B **73**, 100402(R) (2006).
[23] Prellier. W, et.al, *J. Phys.: Condens. Matter* , **17,** R803 (2005)
[24] Bas Van Aken. Et.al, *Nature Materials* **3**, 164 (2004).
[25] Mostovoy , M, *Physical Review Letter* **96**, 067601 (2006).
[26] Rijnders, et.al, *Applied Phys. Letter*, **70**, 1888 (1997).
[27] Palkar V R, John J and Pinto R, *Appl. Phys. Lett,* **80**, 1628 (2002).
[28] Sugawara, et.al, J. *Phys. Soc. Jpn*. **25**, 1553 (1968).
[29] Murakami, et.al, *Applied Phy Lett* **88**, 152902 (2006).
[30] Posadas, et.al, *Applied Physics Letters* , **87,** 17191 (2005).